Geomorphology 229 (2015) 112–124

Contents lists available at ScienceDirect

Geomorphology

journal homepage: www.elsevier.com/locate/geomorph

Submerged karst landforms observed by multibeam bathymetric survey in Nagura Bay, Ishigaki Island, southwestern Japan

Hironobu Kan [a,b,*], Kensaku Urata [c], Masayuki Nagao [d], Nobuyuki Hori [e], Kazuhiko Fujita [f], Yusuke Yokoyama [g], Yosuke Nakashima [h], Tomoya Ohashi [a], Kazuhisa Goto [i], Atsushi Suzuki [d]

[a] Graduate School of Education, Okayama University, Okayama, Japan
[b] Graduate School of Natural Science and Technology, Okayama University, Okayama, Japan
[c] Osaka University of Economics and Law, Yao, Japan
[d] Institute of Geology and Geoinformation, Advanced Industrial Science and Technology (AIST), Tsukuba, Japan
[e] Department of Geography, Nara University, Nara, Japan
[f] Department of Geology, University of Ryukyus, Okinawa, Japan
[g] Atmosphere and Ocean Research Institute (AORI), University of Tokyo, Kashiwa, Japan
[h] Ariake National College of Technology, Omuta, Japan
[i] International Research Institute of Disaster Science (IRIDeS), Tohoku University, Sendai, Japan

ARTICLE INFO

Article history:
Received 31 January 2014
Received in revised form 15 July 2014
Accepted 16 July 2014
Available online 8 August 2014

Keywords:
Submerged karst
Coral reef
Multibeam echosounder
SCUBA
Ryukyu Islands
Japan

ABSTRACT

Submerged tropical karst features were discovered in Nagura Bay on Ishigaki Island in the southern Ryukyu Islands, Japan. The coastal seafloor at depths shallower than ~130 m has been subjected to repeated and alternating subaerial erosion and sedimentation during periods of Quaternary sea-level lowstands. We conducted a broadband multibeam survey in the central area of Nagura Bay (1.85 × 2.7 km) and visualized the high-resolution bathymetric results over a depth range of 1.6–58.5 m. Various types of humid tropical karst landforms were found to coexist within the bay, including fluviokarst, doline karst, cockpit karst, polygonal karst, uvalas, and mega-dolines. Although these submerged karst landforms are covered by thick postglacial reef and reef sediments, their shapes and sizes are distinct from those associated with coral reef geomorphology. The submerged landscape of Nagura Bay likely formed during multiple glacial and interglacial periods. According to our bathymetric results and the aerial photographs of the coastal area, this submerged karst landscape appears to have developed throughout Nagura Bay (i.e., over an area of approximately 6 × 5 km) and represents the largest submerged karst in Japan.

1. Introduction

Evidence suggests that coastal regions shallower than ~130 m have been subjected to repeated alternations between subaerial and marine conditions during the frequent glacio-eustatic sea-level changes that occurred throughout the Quaternary, with extensive environmental change occurring between glacial and interglacial periods (e.g., Yokoyama et al., 2000; Camoin et al., 2004; Fujita et al., 2010). The geomorphology of shallow coastal regions has been modulated by repeated subaerial and submarine processes during glacio-eustatic sea-level change. However, in contrast to the vast knowledge that has been accumulated regarding terrestrial landforms, few previous studies have dealt with shallow seafloor landforms, which represent former terrestrial landscapes modified by present marine processes, from a geomorphological perspective. In this regard, karst geomorphology is no exception, although Taviani (1984) provided some discussion regarding karst-like features on the ocean bottom from various perspectives.

Submerged karst areas are typically recognized by the subaerial exposure of karst landforms in coastal regions. For example, partly submerged tower karsts have been recognized in Ha Long Bay in Vietnam (Waltham and Hamilton-Smith, 2004), Phang Nga Bay in Thailand (Kiernan, 1994), Dweyra Bay and the Blue Grotto in Malta (Paskoff, 2005), and the Rock Islands in Palau (Dieter, 1991). Similarly, submerged karst landforms have been found in Marseille (Collina-Girard, 1996), the Adriatic Coast of Croatia (Surić, 2002), and near Lesbos Island and along the Argolid Peninsula in Greece (Scheffers et al., 2012). In Japan, submerged dolines have been reported only from Minami Island

* Corresponding author at: Graduate School of Integrated Sciences for Global Society, Kyushu University, 744 Motooka, Nishi-ku, Fukuoka 819-0395, Japan.
E-mail address: kan@scs.kyushu-u.ac.jp (H. Kan).

http://dx.doi.org/10.1016/j.geomorph.2014.07.032

(one of the Ogasawara Islands of southeastern Japan), where circular depressions in shallow coastal areas were mapped based on aerial photographs (Hori, 1996). Nevertheless, many previous studies have reported the existence of submerged caves (e.g., Kitamura et al., 2007; De Waele et al., 2009; Surić et al., 2010; Taviani et al., 2012; Mylroie and Mylroie, 2013). These facts suggest the presence of submerged karst features in many coastal areas globally. Moreover, in tropical coral reef areas, antecedent karst underlying postglacial coral reef complexes has been investigated previously and interpreted to control present reef geomorphology (e.g., Purdy, 1974, 1998; Rasmussen and Neumann, 1988; Burke, 1993; Macintyre et al., 2000).

Recent developments in multibeam bathymetric survey technology have enabled the visualization of submarine landforms in three dimensions. For example, this technique has been used to investigate landforms associated with coral reefs (e.g., Webster et al., 2006; Beaman et al., 2008; Abby et al., 2011), bedform structures (e.g., Barnard et al., 2013; Li et al., 2014), tectonic geomorphology (e.g., Tibor et al., 2010; Barrie et al., 2013), glacial features (e.g., Howe et al., 2012), and submerged river landforms (e.g., Harris et al., 2013a). A pioneering study involving the observation of submerged karst by multibeam bathymetric survey was presented by Taviani et al. (2012). That study focused on the Adriatic shelf margin in Italy where eleven submerged dolines with diameters of 50–155 m were found, confirming the presence of thin postglacial deposits covering pre-existing landforms. Similar submerged dolines have been found to the north of the Maltese Islands in the Mediterranean Sea (Micallef et al., 2013). Here, we present the first study to describe a submerged humid tropical karst landscape in Nagura Bay, Ishigaki Island, southern Ryukyu Islands, Japan (Fig. 1A). In particular, we describe the landforms of this region based on a high-resolution bathymetric map with a grid size of 1 m, which we created with reference to observations obtained using our multibeam bathymetric echo-sounding survey combined with SCUBA diving observations.

2. Study area

2.1. Geographical setting

Ishigaki Island is one of the Ryukyu Islands and is located in the northwestern Pacific at latitudes and longitudes of 24°19.8–34.8′N, and 124°13.2–20.5′E, respectively (Fig. 1A). For Ishigaki Island, the average annual mean (1981–2010), monthly maximum, and monthly minimum temperatures are 24.3 °C, 29.5 °C, and 18.6 °C, respectively; the annual rainfall is 2106.8 mm and the average monthly maximum and minimum sea surface temperatures (SSTs) are 29 °C and 23 °C, respectively (Japan Meteorological Agency, 2013). The major western boundary current in the north Pacific, the Kuroshio Current, originates from the Western Pacific Warm Pool (WPWP) and flows through the Ryukyu Islands. Fringing reefs are developed around Ishigaki Island and a 30 × 20 km barrier reef (Sekisei Reef) is developed to the west of the island, lying between Ishigaki and Iriomote Islands. The prevailing wind directions in the vicinity of Ishigaki Island are NNE–NE from September to May and S–SSW

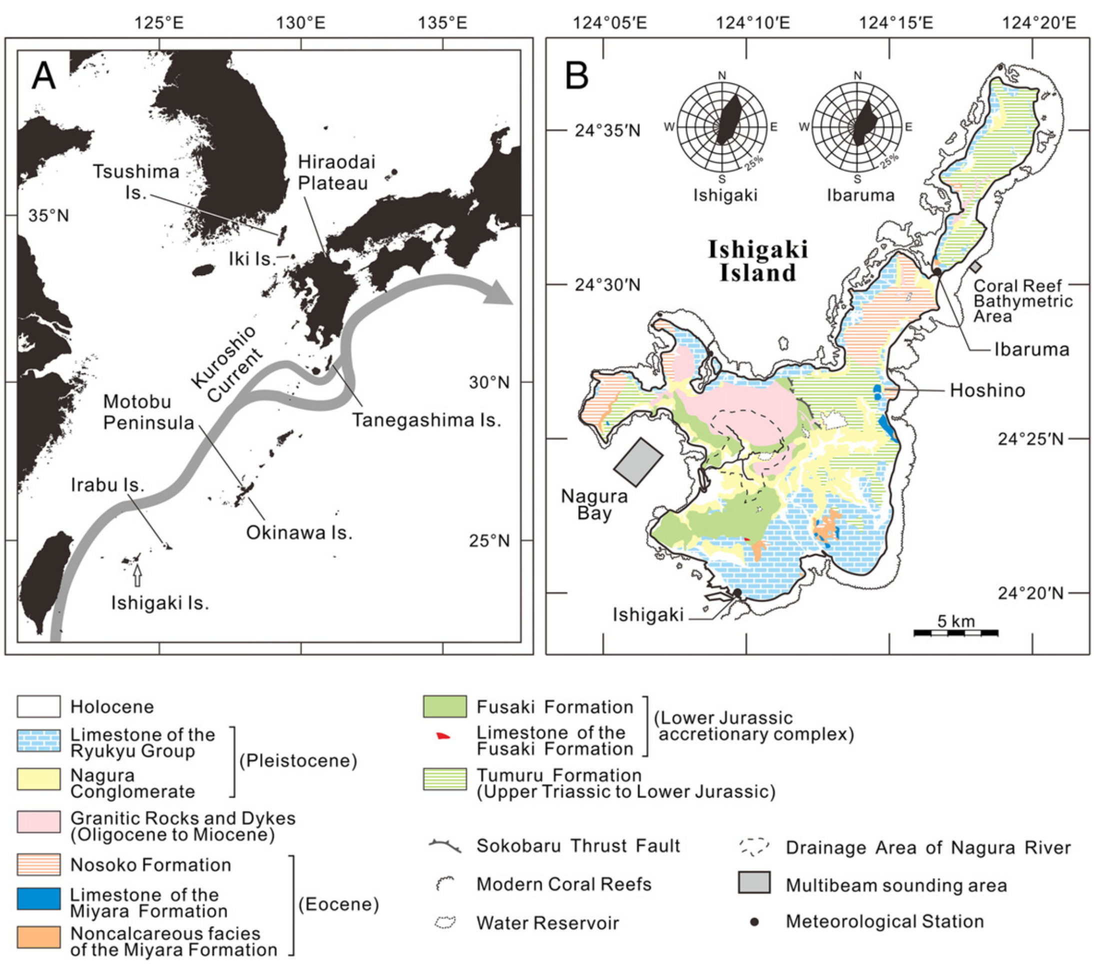

Fig. 1. (A) Location and (B) lithology of Ishigaki Island, showing surveyed area. The flow axis of the Kuroshio Current in (A) illustrates conditions in November 2013, as presented by the Japan Meteorological Agency (2013). Wind roses in (B) have been summarized over the period 1991–2000, as presented by the Ishigakijima (Ishigaki Island) Local Meteorological Observatory for Ishigaki (southwest) and Ibaruma (northeast). Each of the concentric circles in the wind roses represents 5% frequency. The surface lithology in (B) was produced with reference to Nakae et al. (2009).

during June to August (Japan Meteorological Agency, 2013) under the influence of the East Asian monsoon. An average of 7.6 typhoons passed within 300 km of the Ryukyu Islands annually from 1981 to 2010 (Japan Meteorological Agency, 2013), and it has been shown that the monsoon reversal and frequent typhoons in the area were responsible for the development of the high-energy fringing reef environment that surrounds most of the islands in the region (Kan, 2011).

Nagura Bay (which spans 6 km and 5 km in the north–south and east–west directions, respectively) is located on the western coast of Ishigaki Island. Wind roses (Fig. 1B) presented by the Ishigakijima Local Meteorological Observatory (2013) demonstrate that the frequency of the westerly wind is ~1%, suggesting that relatively calm sea conditions are prevalent in Nagura Bay. The environment of Nagura Bay is influenced by the Nagura River and its catchment (Fig. 1B). This river has a mainstream length of 4.6 km and a catchment area of 16.1 km^2 (Ikeda et al., 2009), with a semi-closed river mouth formed by the development of a sand spit and a river mouth wetland that is registered according to Ramsar Convention (Convention on Wetlands of International Importance Especially as Waterfowl Habitat). A mangrove swamp became established at the river mouth ~2 ka, resulting in the accumulation of a thin layer (~30 cm) of mangrove peat (Fujimoto et al., 1995; Miyagi et al., 2003). Additionally, the present environment of Nagura Bay is thought to be influenced by the influx of a terrestrial red soil and nutrient load induced by land-use change to produce sugarcane and pineapple plantations in the drainage area (Ikeda et al., 2009). Distinct submerged groundwater discharge has not been reported around Nagura Bay.

2.2. Geological setting

The geological basement of Ishigaki Island is formed primarily by the Tumuru and Fusaki Formations (Foster, 1965). The Tumuru Formation is an Upper Triassic to Lower Jurassic metamorphic complex (high-pressure low-temperature type) that is composed mainly of pelitic and mafic schists and is distributed throughout the eastern part of the island and on the Yarabu Peninsula at the northern end of Nagura Bay (Fig. 1B). The Fusaki Formation is a Lower Jurassic accretion complex composed primarily of chert, mudstone, sandstone, limestone, and basalt, and is distributed primarily in the southwestern part of the island. The limestone in this formation has yielded Permian fusulinids (Isozaki and Nishimura, 1989). The Tumuru Formation has been thrust upon the Fusaki Formation by the Sokobaru thrust fault and both formations are strongly deformed.

The Middle to Upper Eocene Miyara Formation is a shallow marine deposit, composed of limestones and noncalcareous facies including conglomerates, sandstones, and mudstones, which rests unconformably on the basement Fusaki and Tumuru Formations. The Nosoko Formation is composed of andesitic lavas and tuff and overlies the Miyara Formation conformably. These Eocene rocks have experienced negligible deformation since their deposition (Ujiié, 1996) and it is within the limestone of the Miyara Formation that cone karsts have developed in the eastern part of Ishigaki Island.

After deposition of the Miyara and Nosoko Formations, the study area underwent a period of intense igneous activity. Accordingly, the Oligocene to Miocene geological record (~29.9–21.0 Ma) in this region is characterized by granitic plutonic rocks and dacitic to rhyolitic intrusions (Ujiié, 1996). Subsequently, the Middle Miocene sequence of the Yaeyama Group was deposited in a shallow marine to terrestrial environment. This sequence is composed primarily of conglomerates, sandstones, and siltstones and is distributed throughout the southern Ryukyu Islands. However, these strata are not exposed anywhere on Ishigaki Island; rather, they can be found on Kohama, Iriomote, and Yonaguni Islands, which lie to the west of Ishigaki Island. Most prominently, a limestone layer with a thickness of ~30 m can be observed in the Yaeyama Formation off Miyako Island, 100 km east of Ishigaki Island (Tsuburaya and Sato, 1985).

After the second phase of extension of the Okinawa Trough commenced ~2 Ma (Sibuet et al., 1987), the Ryukyu Islands experienced remarkable development of coral reefs that accumulated to form the Pleistocene limestone of the Ryukyu Group. This limestone is composed of shallow water (0–50 m depth) coral framestone and deep water (50–150 m depth) rhodolith and *Cycloclypeus*–*Operculina* rudstone covering the insular shelf (Nakamori, 1986; Nakamori et al., 1995; Iryu et al., 1998). Around Ishigaki Island, a relatively thin coral reef limestone formed after 0.41 Ma (Iryu and Matsuda, 2010), when it grew on a Pleistocene conglomerate known as the Nagura Gravel (Foster, 1965). $^{230}Th/^{234}U$ ages and altitudes of in situ *Porites* corals from the upper part of the Pleistocene coral reef limestone have provided ages of 118.5 ± 2.0 ka at 1.3 m at Ibaruma (in the northern part of Ishigaki Island) and 119.9 ± 2.0 ka at 15 m at Arakawa (in the southern part of Ishigaki Island), permitting their assignment to Marine Isotope Stage 5 (MIS5). Therefore, this limestone is best assigned to the last interglacial period (Marine Isotope Stage 5e; hereafter, MIS5e). Based on these ages and altitudes, uplift rates after MIS5e have been estimated to be -0.01 to 0.03 m ka^{-1} and 0.1 to 0.4 m ka^{-1} in the northern and southern parts, respectively, of Ishigaki Island (Yamada et al., 2007). Taking this northward tilting of Ishigaki Island into account, an intermediate uplift rate is presumed for Nagura Bay, which is located in the middle part of the island.

3. Methodology

3.1. Multibeam survey

A broadband multibeam echosounder (Sonic 2022, R2 Sonic, LLC) and its accessory system were used for this research. The Sonic 2022 has a variable ultrasonic frequency of 200–400 kHz and a 60 kHz signal bandwidth throughout its frequency range. It has 256 ultrasonic beams and selectable swath coverage of 10–160°. The typical ultrasonic beam widths parallel and orthogonal to the direction of travel are within one degree of each other when an ultrasonic frequency of 400 kHz is selected. For the present study, the accessory system of the Sonic 2022 consisted of a VS111 GPS compass system with A20 and A30 antennas (Hemisphere Inc.) combined with a dynamic motion sensor (DMS-10, Teledyne TSS Ltd.), a sea surface sound velocity sensor (miniSVS, Valeport Ltd.), a sound velocity profiler (MicroSVP, AML Oceanographic Ltd.), a sonar interface module (SIM), a junction box, and an operation PC with hydrographic survey software (HYPACK2010). The theoretical vertical resolution for the entire frequency range of the Sonic 2022 is 1.25 cm; however, the actual vertical resolution has been estimated to be 5–10 cm, because the vertical resolution depends on the measurement accuracy of both the accessory system and the echosounder (Nagao et al., 2011). The HYPACK2010 software was used for both hydrographic survey and data processing. Because complex undulations of submarine topography are known to exist in the surveyed area, we did not use the automatic noise filters provided in HYPACK2010. Rather, we identified noise by determining geomorphological patterns and continuity and removed the noise from every beam profile manually. The JGD2000/Japan Plane Rectangular CS XVI coordinate system was adopted for Ishigaki Island. IVS3D Fledermaus (Interactive Visualization Systems Inc.) was used for three-dimensional visualization with a grid size of 1 m and as an aid for description.

Multibeam bathymetric surveys were conducted in a rectangular area spanning 1.85×2.7 km in the central part of Nagura Bay (Fig. 1B). The surveyed area was defined by a rectangle with four corners: 24°25′13.4″N, 124°06′32.4″E (northwest); 24°24′36.6″N, 124°07′20.1″E (northeast); 24°23′30.0″N, 124°06′17.9″E (southeast); and 24°24′08.3″N, 124°05′29.3″E (southwest). The coastal areas within the bay were too shallow to conduct any surveys. Because the observed geomorphology of Nagura Bay was distinct from other coral reef areas around Ishigaki Island, an additional bathymetric survey was conducted for coral reef morphology of reef edge and reef slope areas of northeastern Ishigaki Island to enable comparison of the bathymetric results for Nagura Bay with typical coral reef geomorphology. In general, the ultrasonic frequency of 400 kHz was selected for bathymetric survey, however, we adopted 200 kHz in the southwestern (i.e., oceanward) third of the Nagura Bay area owing to the occurrence of occasional weak reflections produced by partially distributed soft bottom sediments and to increase swath width. Overlap of at least ~20% (typically ~50%) was implemented throughout the bathymetric survey to ensure 100% coverage of the surveyed area.

3.2. SCUBA observations

The ground truthing was achieved by SCUBA diving observations at seven sites down to a depth of 40 m in November 2011. Surface features (sediments, rocks, coral assemblages) were also observed by SCUBA diving. Underwater photographs were taken using a Nikon D300 with a frame-filling fisheye lens (AF DX Fisheye Nikkor, 10.5 mm, f/2.8G) mounted in a Nauticam housing.

3.3. Sampling and analysis of geological materials

During the SCUBA diving surveys, we collected three bedrock carbonate samples using a hammer and chisel from the overhanging walls at the edge of the submarine plateau to define the main lithologies affected by karst processes. Two sediment samples were also collected for a preliminary description of sediment types draping the bottom of the submarine canyon in the central part of the study area.

Optical microscopy of bulk samples was conducted using a binocular stereoscopic microscope. X-ray diffraction (XRD) analyses to determine the mineralogy of rock and sediment samples were conducted using a Rigaku MiniFlex II X-ray diffractometer. Quantitative analyses of minerals were undertaken using powder diffraction analysis software (Rigaku PDXL) employing the reference intensity ratio (RIR) method with reference to the mineralogical database of the International Center for the Diffraction Data (ICDD).

In November 2013, we started drilling down to 60 m depth at 24°24′32.5″N, 124°06′42.3″E. We discuss here some preliminary information, because this is, to date, the only source of borehole information for the entire Nagura Bay area.

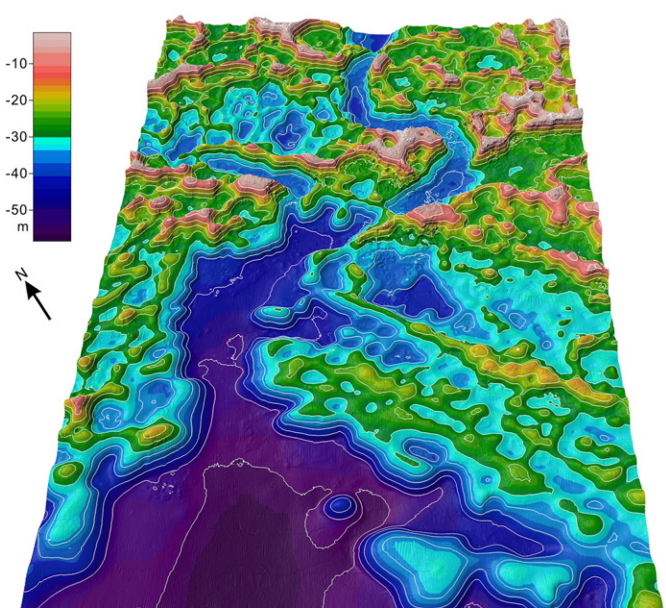

Fig. 2. Multibeam bathymetry of Nagura Bay. A high-resolution model of our bathymetric results, visualized with a horizontal grid size of 1 m. Color scales show depths. Contours indicate 5 m isobaths. Vertical exaggeration is times 3.

4. Results

4.1. Seafloor landforms

The bathymetric results obtained for the central part of Nagura Bay (spanning 1.85 × 2.7 km) are presented in Fig. 2. The depth of the surveyed area is within the range 1.6–58.5 m. In general, the seafloor landforms of Nagura Bay are characterized by large, frequent undulations (~30 m) with numerous depressions (represented by closed contours in the figure). The undulations decrease in the seaward (i.e., southwestward) direction, such that a flat seafloor without closed depressions appears below 40 m.

The terrestrial karst landscapes break up the integrated and scalable patterning typical of fluvial systems by encouraging the development of small centripetal drainage basins and closed depressions exhibiting irregular patterning (Jennings, 1985). The seafloor morphology of Nagura Bay resembles that associated with terrestrial karst landforms and may be attributed to a submerged karst that developed during a sea level lowstand. Although there may be some uncertainty attached to applying terminology related to subaerial geomorphology to the seafloor landforms, as suggested by Taviani (1984), we tentatively apply the terminology of terrestrial karst landforms to describe the submarine landforms of Nagura Bay because no terminology exists to describe either the landforms found in the coral reef or the geomorphology of the seafloor in this context. In particular, we observed five types of karst

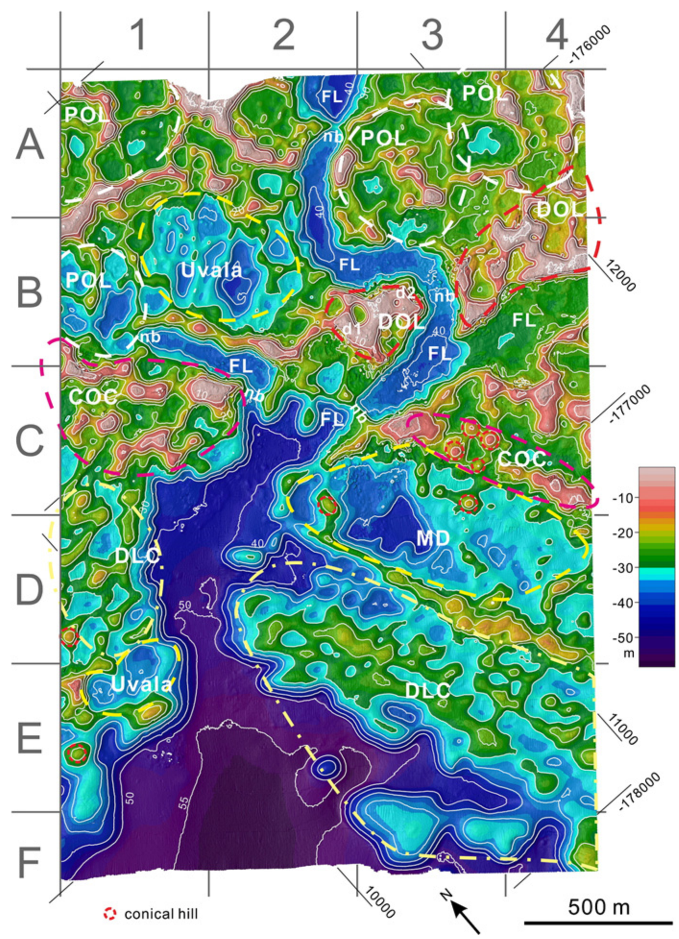

Fig. 3. Geomorphological interpretation of Nagura Bay. A plan view with 5 m contours, with locations represented in the JGD2000/Japan Plane Rectangular CS XVI coordinate system. Grid lines are drawn at 500 m intervals to identify different geomorphological sites. Color scales show depths. FL: fluviokarst, nb: natural bridge, DOL: doline karst, COC: cockpit karst, POL: polygonal karst, MD: mega-doline, DLC: dissected low-relief cockpit karst. d1, d2: individual doline cited in the text.

landform in the surveyed area (Fig. 3) and suggest that these features may represent the styles and stages of karst development.

4.1.1. Fluviokarst

A meandering valley was observed to traverse the study area from northeast to southwest. This valley is interpreted as the trace of a paleo-river (i.e., forming a fluviokarst landscape). The fluviokarst landscape here is characterized by crescent-shaped closed depressions with widths of 150–200 m, with a maximum depth of 41 m occurring in the deepest parts of the valley (i.e., in regions A2, B2, B3, and C3 in Fig. 3). In the upper and lower reaches of the stream, the depression has lengths of ~800 m (A2–B3) and ~500 m (B3–C3), respectively. In this region, the steepest gradients are found on the undercut slopes of the meandering valley. The transversal ridges separating the upstream and downstream regions of the fluviokarst depressions may represent the remnants of natural bridges, where the upstream and downstream parts may have been connected previously by a lower corridor.

A shallower valley is observed beside the main valley in the B3–B4 regions. This valley has a maximum depth of ~30 m and a width of ~200 m. An isolated mound with diameter of 50 m remains in the central part of the valley (i.e., at B4). Furthermore, another fluviokarst region with length and width of 500 m and 150 m, respectively, is developed at B1–B2, with natural bridges dividing its western and southeastern reaches. However, such valleys with natural bridges do not appear to exist at depths greater than 40 m in Nagura Bay, where a flat seafloor extends offshore from C2 to E2.

4.1.2. Doline karst

Two submarine plateaus (i.e., eastern and western plateau) with concordant ridge elevations that are separated by a fluviokarst depression are observed in shallow water between B2 and B4 (i.e., water depths of less than 8 m). These plateaus have a width of 200–300 m. Enclosed depressions on the plateau, referred to here as dolines, exhibit bowl-shaped basin forms with flattish floors.

The top depth of the western plateau located in B2 and B3 is in the range 5–7 m. Two dolines are developed on this plateau: one has diameter and depth of 100 m and 18 m, respectively (d1 in Fig. 3), whereas the other has diameter and depth of 30 m and 8 m, respectively (d2). Additionally, we found the northern and western edges of this plateau to be fringed by numerous dolines with diameters of 80–100 m.

The upper surface of the eastern plateau is less extensive than that of the western plateau. The dolines of the eastern plateau typically exhibit diameters and depths of ~100 m and ~15 m, respectively, although a small doline (50 m diameter, 10 m depth; d3) was found in the central part of the plateau. Similarly, the dolines found in Nagura Bay were mostly ~100 m in diameter, although smaller dolines with diameters of ~30–50 m have also been established on the upper surfaces of the submarine plateau in this region.

4.1.3. Cockpit karst

The cockpit karst is described as the “egg-box” style of polygonal karst, which is characterized by steep-sided enclosed lobate depressions surrounded by residual hills, typically developed in Cockpit Country in Jamaica (Day and Chenoweth, 2004). Two cockpit karst areas are recognized in Nagura Bay (C1–C2 and C3–C4), adjacent to the central fluviokarst region. These areas exhibit typical cockpit karst forms, with “egg-box” depressions and intervening conical hills. In the eastern areas (C3–C4), conical hills (although some of the tops are flat, with the relief appearing to be mesa-like) and enclosed lobate depressions are aligned with a ridge extending in the NNW–SSE direction; four distinct conical hills (with diameters and heights of 60–100 m and 10–15 m, respectively) are observed in this area. Conversely, in the western area (C1–C2), typical “egg-box” depressions with diameters of 70–100 m are apparent. The relief formed by undulations between the tops of the conical hills and the bottoms of the intervening depressions is typically 20–25 m, although the tops of the conical hills in the western area (C1–C2) are typically shallower than those in the eastern area (C3–C4).

4.1.4. Polygonal karst with central hill

Submarine landforms resembling polygonal karst with a cellular network are recognized in the surveyed area (Fig. 3). Although the above-mentioned cockpit karst is a type of polygonal karst, this additional category of polygonal karst is characterized by the relative lack of conical hills. Five areas within the study area exhibit polygonal karst features, as follows. (1) Five narrow saddles extend radially in different directions from the central residual hill in A1. These saddles form topographic divides between adjoining depressions, producing a pentagonal pattern in plan view. The top of the central hill lies at a depth of 6.2 m, whereas the saddles of the radial narrow ridges are at depths of 13.5–23.1 m. The adjoining depressions exhibit a maximum depth of 31.85 m and typically have diameters of ~100–200 m, as with the dolines in Nagura Bay. Small conical hills with heights of 3–4 m remain in some depressions. Although the northern margin of this polygonal karst lies outside the bathymetric survey area, we believe that the diameter of this formation may be ~500 m based on the distance between the central hill and the peripheral ridges of the depressions. (2) A polygonal karst with a diameter of ~500 m is observed in the B1 area. The depth of the top of the central hill is 19.4 m and the depression exhibits a maximum depth of 39.3 m. Two distinct radial narrow saddles extend from the central hill; however, all other saddles are discontinuous. (3) The polygonal karst located in the A3 area exhibits a diameter of ~500 m, corresponding to other polygonal karsts in Nagura Bay. The central part of this polygonal karst consists of a series of complex hills, the highest of which exhibits a square shape in plan view (100 × 80 m). The top and bottom depths of this hill are ~5 m and ~27 m, respectively, whereas the depth of the top of the central bean-shaped ridge (120 × 60 m in plan view) is 8.9 m. Three other conical hills (with diameters and heights of 40–50 m and 10–15 m, respectively) constitute the remainder of the central hill complex. The depressions between these conical hills are ~80 m in diameter. This central hill complex resembles the cockpit karst in the C1 area, although larger depressions (~100–200 m diameter) are recognized around the central hill complex. The maximum depth of the depressions in this area is 31.7 m, and the southwestern depression is connected to the adjoining fluviokarst. (4) A similar polygonal karst can be seen in the A4 area, to the east of the A3 polygonal karst.

4.1.5. Uvalas and mega-dolines

The large compound closed depressions are evident within the study area (Fig. 3). (1) A large depression of 650 × 400 m has formed around the B1–B2 area and is subdivided internally into smaller second-order depressions with diameters of ~50–300 m. This arrangement resembles an uvala (i.e., compound doline), which is typically formed by the enlargement and merging of individual dolines (Ćalić, 2011). The largest and deepest (maximum depth: 40.9 m) depression is located in the southern part of this uvala. A small cone with a height and diameter of ~50 m and ~3 m, respectively, remains in the central part of the uvala (i.e., at the eastern end of the B1 area) and second-order depressions are located around the central cone. Based on the distribution of the second-order depressions, we assume that the original form of this uvala was a polygonal karst. Another uvala with dimensions of 360 × 180 m has formed around the D1–E1 area. (2) A large depression (tentatively referred to as a mega-doline) with a length and width of 1000 m and 500 m, respectively, is seen between the C2 and D4 areas. The long axis of this depression is oriented NNW–SSE, corresponding to the long axis of the above-mentioned uvala. However, in contrast to the uvala, second-order depressions are indistinct in this mega-doline. Six isolated conical hills remain in this area, forming topography similar to that expressed by the terrestrial karst landform known as “hum” in the Dinaric classical

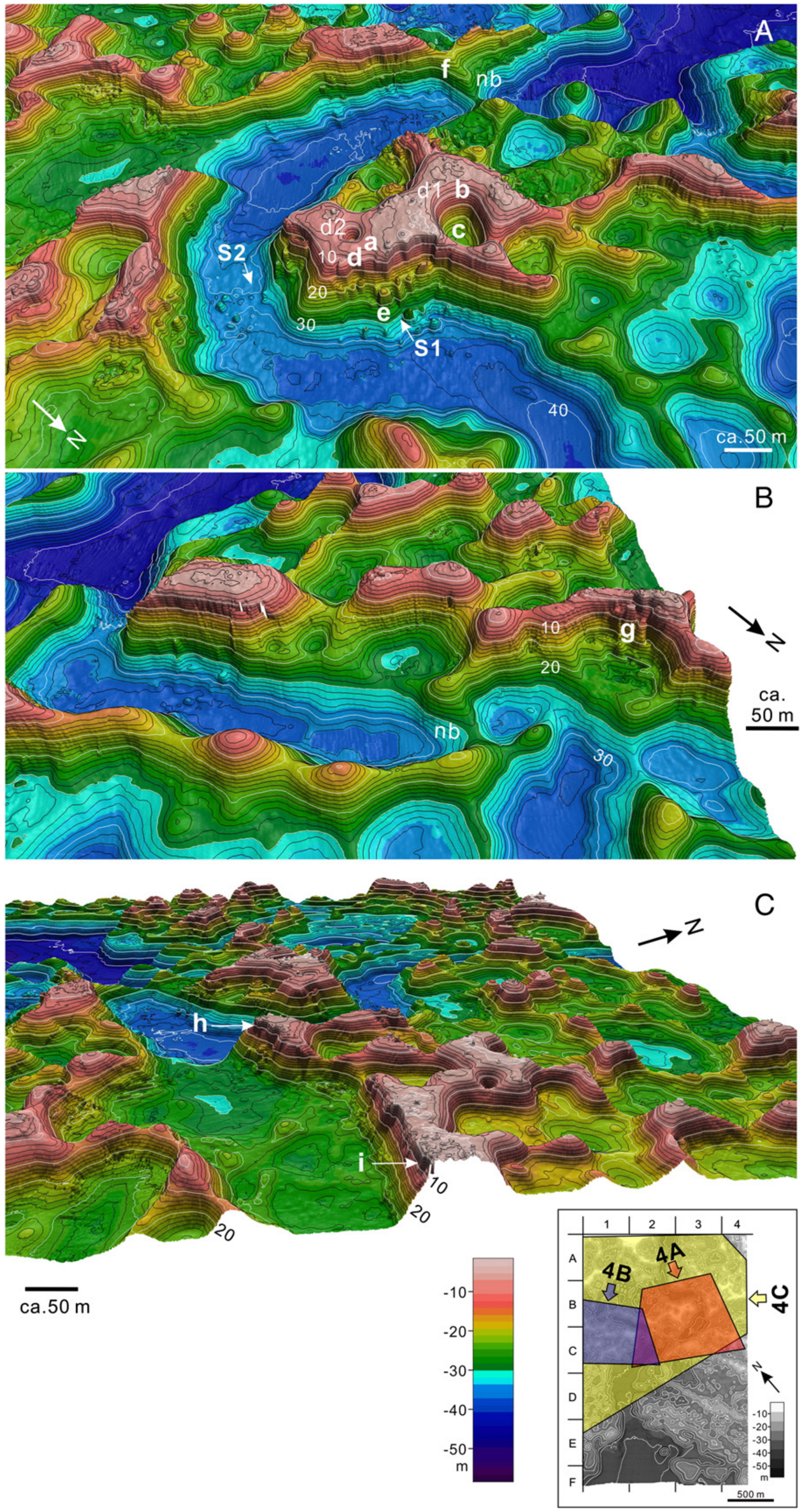

Fig. 4. Three-dimensional views of submerged karst in Nagura Bay showing observation and sampling sites. Contours indicate 5 m (white) and 1 m (black) isobaths. Color scales show depths. Scale bars represent approximately 50 m. Panels show (A) doline karst and fluviokarst viewed from the northeast, (B) polygonal karst (right) and fluviokarst (left) viewed from the northeast, and (C) fluviokarst viewed from the southeast. d1 and d2: dolines corresponding to Fig. 3, nb: natural bridge, a–i: photographic sites illustrated in Fig. 5. Sampling sites of rocks and surface sediments (as shown in Table 1) are indicated by h/i and S1/S2, respectively. The map shown in the bottom right panel shows the areas of Fig. 4A (red), 4B (blue), and 4C (yellow) overlaid on a plan view corresponding to Fig. 3. Arrows indicate the direction of three-dimensional views. Vertical exaggeration is times 3.

karst. These solitary conical hills appear to be the remnants of the conical hills typical of polygonal karst.

4.1.6. Low-relief cockpit karst

Low-relief cockpit karsts are distributed in two seaward areas of the study area: the D2–D4 and C1–E1 areas (Fig. 3). The tops of the conical hills in these regions lie below 20 m depth, and the slopes of these hills are gentler than those of the cockpit karst found around areas C1 and C3–C4. This low-relief cockpit karst constitutes the outer margin of the submerged karstic landforms in Nagura Bay.

4.2. SCUBA observations

SCUBA diving surveys were conducted for geomorphological and sedimentological observations in three areas: the central submarine plateau, the western polygonal karst, and the edges of the eastern submarine plateau.

The surface of the central submarine plateau (Fig. 4A) at a water depth of ~5–6 m was found to be covered by living corals that consist primarily of large free-living fungiids (Fig. 5A) and branching corals. The interior slope of the d1 doline (~100 m in diameter) was found to be covered by living foliaceous corals and free-living fungiids and

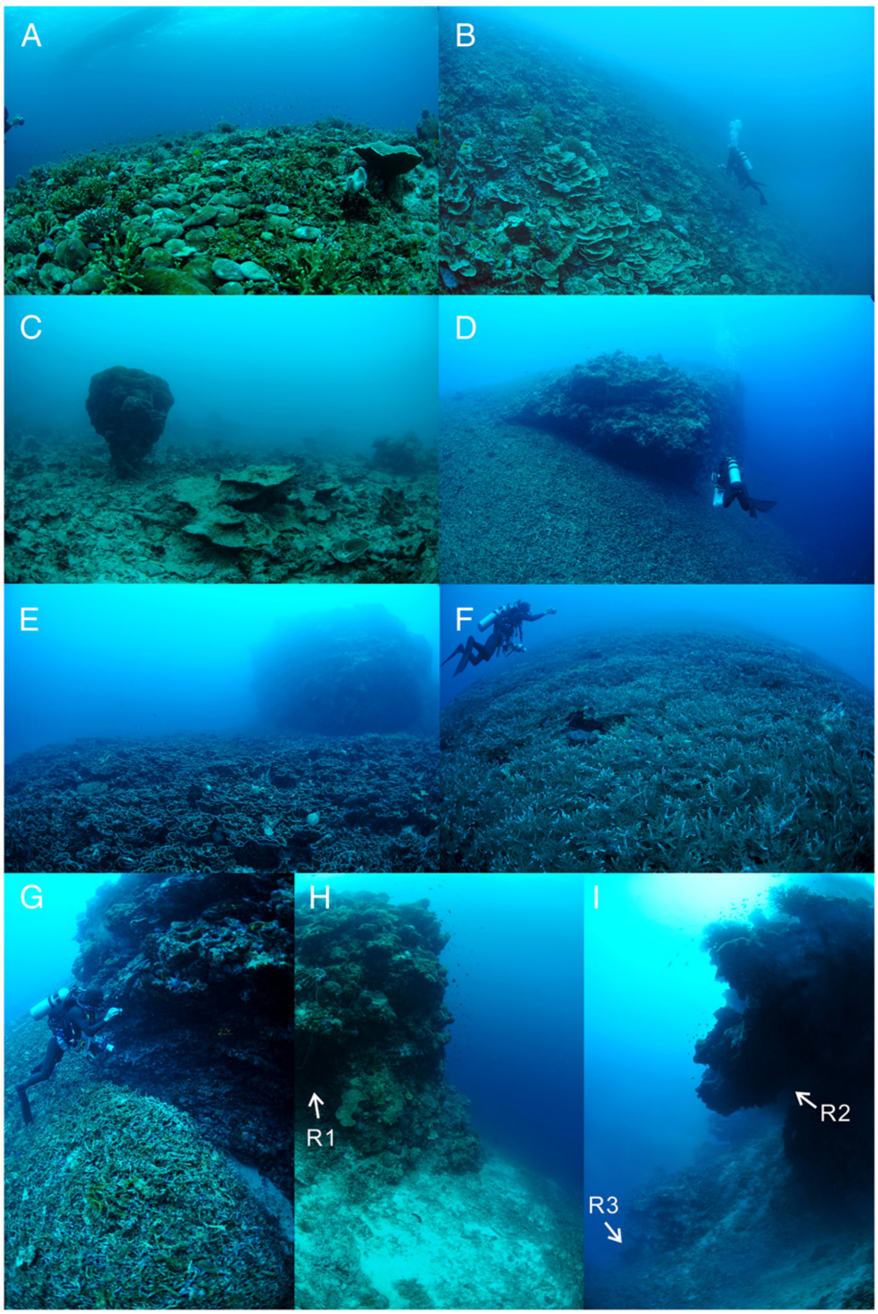

Fig. 5. SCUBA diving observations of geomorphology and seafloor conditions in Nagura Bay. Photographic sites are indicated in Fig. 4. A: Top surface of the submarine plateau covered by living solitary and branching corals (depth: 5 m). B: Foliaceous *Montipora* in the middle of an interior slope of doline d1 (depth: 15 m). C: Living coral head at the bottom of doline d1 (depth: 23 m). D: Edge of the submarine plateau where branching coral rubble forms talus creeps that extend toward the fluviokarst valley (depth: 10 m). E: Monospecific communities of foliaceous coral (depth: 22 m). F: Large thicket of branching *Acropora* sp. (depth: 23 m). G: Accumulation of branching coral rubble with height of ~1.5 m at the foot of an overhanging wall (depth: 15 m). H: Upper steep slope and lower slope covered by reef talus along the slope of the fluviokarst valley (depth: 12 m). I: An overhanging wall at the top of the fluviokarst valley (depth: 10 m). All photographs were taken by H. Kan in November 2011.

branching corals and their rubble at the midslope to baseslope (Fig. 5B). The bottom of the doline lies at a water depth of 24 m; here, the presence of a living coral that widens toward its top (Fig. 5C) suggests that the bottom of the doline has experienced waveless conditions for an extended period of time. Reef sediments consisting primarily of branching coral rubble were found to have formed talus creep deposits along the northern edge of the submarine plateau (Fig. 5D). Furthermore, some monospecific living coral communities consisting of branching or foliaceous corals (Fig. 5E) were found in the midslope region, and a grayish white carbonate mud with rubble has accumulated on the bottom of the valley. We also discovered a large living branching coral community dominated by *Acropora* (Fig. 5F) extending over a natural bridge lying to the south of the central submarine plateau (C3 in Fig. 3; f in Fig. 4A).

The interior slope of the polygonal karst in the B1 area (Fig. 4B) is particularly steep at water depths shallower than 24 m. Along the upper steep slope, branching coral rubble has accumulated to a thickness of ~1.5 m at the foot of an overhanging wall (Fig. 5G). Living large coral communities here include laminar *Montipora* sp., branching *Acropora*, and foliaceous corals distributed along the gentle slope at 24–28.7 m.

At the edge of the eastern submarine plateau (Fig. 4C), the upper slopes are formed by very steep or overhanging walls that extend to ~12 m and ~15 m depth at sites “h” (Fig. 5H) and “i” (Fig. 5I), respectively. Below these walls, modern reef sediments form talus that covers the slope surface. No corrosional features were observed during our SCUBA surveys.

4.3. Surface lithology and sedimentology

Two bottom sediment samples (S1 and S2 in Table 1) were collected from two sites within the main valley (S1 and S2 in Fig. 4A) at depths of 30.8 m (S1) and 35.2 m (S2). The sediments in these samples were found to consist of grayish white carbonate mud with rubble of *Halimeda* and fragments of coral–algal framestone. Three rock samples (R1–R3 in Table 1) were collected from the overhanging walls (Fig. 6) at the edge of submarine plateau (sites “h” and “i” in Fig. 4C). The depths of the sampling sites were 12.7 m, 8.3 m, and 15.8 m for R1, R2, and R3, respectively. In terms of lithofacies, we classed these samples as coral–algal boundstones (R1 and R3) and a carbonate grainstone (R2) (Fig. 6). Owing to the lack of evidence of subaerial exposure, we believe such carbonates to have been formed recently. The detected mineralogies of these samples consist of aragonite and high-magnesium (high-Mg) calcite minerals (Table 1).

In general, the rock and sediment samples described here indicate that the upper lithofacies of Nagura Bay consist of recent coral reef and reef sediments that have accreted or accumulated after the postglacial sea level rise. The maximum thickness of postglacial reef around Ishigaki Island has been reported to be 22 m for the fringing reef along the northeastern coast of the island (Hongo and Kayanne, 2009) and ~20 m for the barrier reef developed 2–10 km southwest of Ishigaki Island (Kan and Kawana, 2006). Because the top of the submarine plateau lies at ~5 m water depth, the recent coral–algal boundstone collected from 15.8 m water depth suggests that more than 10 m thickness of reef has been accreted in this postglacial period. Smaller karst features at the meter scale (i.e., less than 10 m), such as solution runnels, were not observed in Nagura Bay, likely because they were buried by the postglacial reef complex.

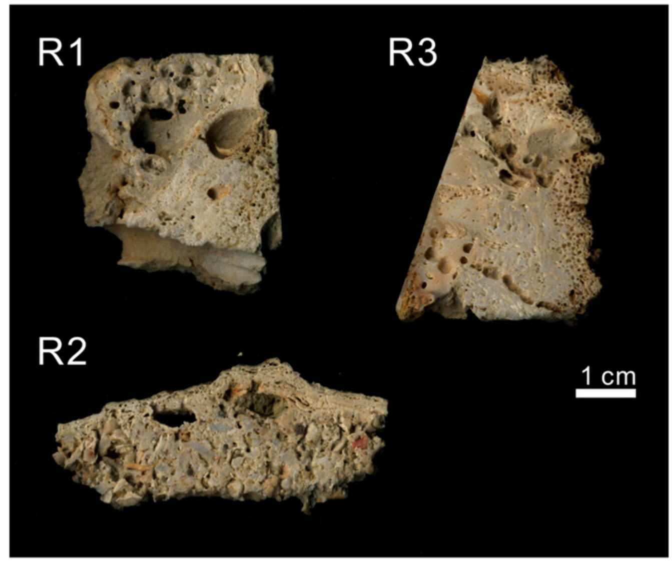

Fig. 6. Rock samples collected from the upper layer of submerged karst in Nagura Bay. (R1) coral–algal boundstone collected from site “m” at 12.7 m depth. (R2) carbonate grainstone collected from site “n” at 8.3 m depth. (R3) coral–algal boundstone collected from site “n” at 15.8 m depth. Sampling sites (as shown in Table 1) are indicated in Figs. 4C and 5H/I.

5. Discussion

5.1. Difference from coral reef geomorphology

Because the surface lithology of Nagura Bay is formed by the modern reef structure, it is important to discuss how the geomorphology of Nagura Bay is distinct from that of coral reefs. In general, the coral reef geomorphology of Ishigaki Island includes a reef crest, shallow lagoon, and reef slope. This sea level reef exhibits a zonal geomorphology in which the reef crest (with a width of ~200–300) has developed 500–1000 m offshore, oriented along the coastline of the island (e.g., Goto et al., 2010). The shallow lagoon (~3 m deep) has formed between the reef crest and shore. These zonal reef features around Ishigaki Island were built up ~4 ka (Yamano et al., 2001; Kan and Kawana, 2006; Hongo and Kayanne, 2009); that is, they were generally formed when the reef reached sea level after the middle Holocene and matured during the late Holocene in the Ryukyu Islands (Kan, 2011). In particular, the spurs and grooves making up the smaller reef features at present were developed under stable sea level during the late Holocene owing to reef flat accretion at the reef edge (Kan et al., 1997; Kan, 2011). Such distinct zonal reef features at such large scales (i.e., hundreds of meters in the horizontal direction) have not been reported previously for offshore reefs.

Fig. 7 illustrates a 500 × 500 m area of the submarine landscape in Nagura Bay (Fig. 7A; around the C1 area in Fig. 3) alongside the coral reef morphology of the reef edge and reef slope areas along the northeastern coast of Ishigaki Island (Fig. 7B) at the same scale. In the latter,

Table 1
Mineralogical composition of sediment and rock samples collected from Nagura Bay.

Sample number	Site in Fig. 4	Depth (m)	Mineralogical composition (%)			Lithofacies
			Aragonite	High-Mg calcite	Others	
S1		30.8	38.8	61.2	0.0	Sediment
S2		35.2	41.6	58.4	0.0	Sediment
R1	h	12.7	77.6	22.4	0.0	Coral–algal boundstone
R2	i	8.3	39.7	60.3	0.0	Grainstone
R3	i	15.8	89.7	10.3	0.0	Coral–algal boundstone

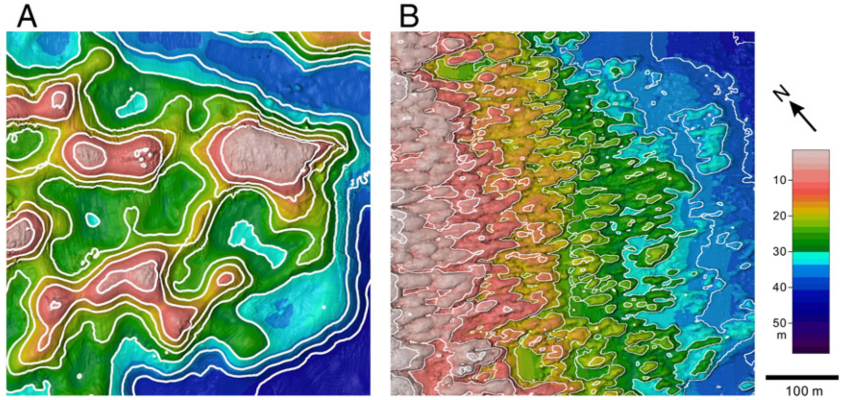

Fig. 7. Geomorphology of submerged karst and coral reef at Ishigaki Island. (A) Submerged karst in Nagura Bay. (B) Coral reef around northeastern Ishigaki Island (see Fig. 1B). Bathymetric results are in plan view and cover areas of 500 × 500 m, visualized for a horizontal grid size of 1 m. Color scales show depths. Contours indicate 5 m isobaths.

the depth is in the range 2–40 m, and distinct spurs and grooves have developed with long axes parallel to wave orthogonals. This reef topography can be considered typical of the Ryukyu Islands. Spur widths vary with water depth: widths are 20–40 m, 10–20 m, and ~10 m at the reef edge, below 10 m water depth, and at depths of 25–30 m, respectively. Conversely, spur lengths are relatively constant with depth and are predominantly 50–70 m. The relative heights of spurs with respect to the intervening grooves are ~5–10 m at all depths down to the 30 m isobath. This pattern of reef geomorphology corresponds to the marine conditions that prevailed during the middle to late Holocene; in particular, the arrangement of spurs and grooves corresponds to wave orthogonals.

In contrast to the reef geomorphology described above, the bathymetric map of Nagura Bay (Fig. 7A) is characterized by large geomorphological units with gently curved isobaths and large undulations. The dominant horizontal scale of the geomorphology of Nagura Bay is greater than 100 m, similar to the ~100 m diameters of dolines but much smaller than the ~500 m diameters observed for polygonal karsts. Based on our results, the submarine landscape of Nagura Bay is entirely distinct from the geomorphology of the present coral reef in terms of both spatial scale and pattern. Thus, although the submerged landforms in Nagura Bay are covered by the recent reef complex (rocks and sediments), the general outlines of landforms at the scale of hundreds of meters have been preserved.

5.2. Present-day marine environment in Nagura Bay

Nagura Bay is located on the western coast of Ishigaki Island, where the wave intensity is lower than elsewhere around the island. Moreover, the distance of 5 km from the offshore area to the bayhead produces a gradual decrease of wave intensity toward the shore, and the bottom of the drowned doline experiences a semi-enclosed and waveless environment due in part to the protected nature of the bay (e.g., Fig. 5C). The large undulations are another remarkable feature of the submarine landscape of Nagura Bay: the submarine plateaus at ~5 m water depth lie adjacent to valleys at ~40 m water depth. Such a configuration is relatively unique in coral reef geomorphology, even in comparison to the morphology of the reef system around the rest of Ishigaki Island. Owing to these large undulations and the terrestrial influence, underwater irradiance tends to be lower in Nagura Bay than in other coral reef areas around Ishigaki Island. Based on these gradients in physical properties (i.e., wave properties and irradiance), we assume the existence of various environments and associated biota in Nagura Bay.

It has been reported that the living coral coverage of only ~10% in Nagura Bay is composed primarily of massive (hemispherical) coral *Porites* sp. (Nature Conservation Bureau, Ministry of the Environment, 2002). This coverage ratio is the lowest observed throughout the fringing reefs around Ishigaki Island. However, we observed large coral communities during our preliminary SCUBA observations (e.g., Fig. 5E, F). In particular, abundant corals with branching and solitary growth forms were found living on top of the central submarine plateau. Furthermore, plentiful living corals with branching, foliaceous, and laminar growth forms were also observed on the intermediate gentle slopes at ~20–30 m depth in regions of steep slopes beside fluviokarst valleys or polygonal karst slopes, with coral rubble covering the steep slopes as talus and muddy sediments accumulated on the bottoms of valleys and depressions. In general, reduced irradiance has been shown to give rise to extensive mesophotic coral communities in shallower environments, typically at depths of 30–150 m (Lesser et al., 2009; Slattery et al., 2011), and such conditions are thought to be important in forming refuges for shallow coral communities (Bak et al., 2005; Bridge et al., 2013; Harris et al., 2013b). Thus, the abundant living corals found along the deeper gentle slopes in Nagura Bay may play an important role in supporting the regional coral reef ecosystem.

5.3. Paleoenvironment in the glacial period around Ishigaki Island

The development of karst landforms is closely related to regional climate variables such as temperature and precipitation (e.g., Daoxian, 2013). However the karst morphology in coral reef areas may reflect past climatic conditions, particularly those that prevailed during sea-level lowstands (e.g., Purkis et al., 2010). Cockpit karst typically develops in humid tropical or subtropical climates and is morphologically distinct from most temperate dolines as suggested by Lehmann (1936, in Ford and Williams., 2007). The present climate of Ishigaki Island provides conditions favorable for the development of cockpit karsts, as indicated by Zhu et al. (2013).

The climate of the Ryukyu Islands is influenced by the warm Kuroshio Current of the major western boundary current and the East Asian monsoon. In contrast to present conditions, where the Kuroshio Current flows through the Ryukyu Islands, the results of deep sea drilling have suggested that this current was weakened during the last glacial period such that it did not enter the East China Sea fully (e.g., Diekmann et al., 2008). Reef growth during the last glacial period has been constrained by drilling of the island shelf off Irabu Island in the southern Ryukyu Islands (Sasaki et al., 2006). This reef grew 22–15 ka at the present depth of 126.2–123.2 m and was drowned by the subsequent postglacial sea level rise. Massive faviid corals were the dominant species in the drowned reef, which resembled the higher latitude coral reefs reported for the Iki and Tsushima Islands in Japan at 34°N (Yamano et al., 2012). The oxygen isotope and Sr/Ca records of a faviid coral of 16.17 ka suggest that the paleo-SSTs were ~5 °C lower than present-day SSTs, whereas a stronger winter monsoon and weaker summer monsoon have been inferred based on sea surface salinity (SSS), which was at least ~0.2‰ higher than present-day SSS (Mishima et al., 2009). Furthermore, an ocean drilling core obtained from the Ryukyu Trench slope off the south of Ishigaki Island (International Marine Past Global Changes Study (IMAGES), core MD01-2398, located at 23°59.51′N, 124°24.76′E) also indicates MIS-2 SSTs that were ~2 °C and ~5 °C lower in summer and winter, respectively, than present-day SSTs (Ujiié and Ujiié, 2006).

Present-day winter SSTs of 23 °C and 19 °C have been reported for Ishigaki and Tanegashima Islands, respectively; the latter is located at 30°N, in the northern Ryukyu Islands (Japan Meteorological Agency, 2013). Coral facies and paleo-SSTs indicate that the environment of the southern Ryukyu Islands during the last glacial period resembled present-day conditions at latitudes of 30–34°N. Thus, the submerged karst in Nagura Bay would have developed under a climate that was slightly cooler and drier than the present day but still humid tropical or subtropical.

Corrosion rates of 87.3–102.6 mm ka^{-1} have been reported for tropical and subtropical karst areas in China (Zhu et al., 2013), and similar rates have been observed or calculated (using theoretical denudation equations) for other regions globally (Gunn, 2013). Assuming that dissolution does not always contribute only to direct lowering of the land surface but is also involved in the development of epikarst (Gunn, 2013), and considering the timescales involved in limestone corrosion, the development of the karst landforms in Nagura Bay likely proceeded throughout multiple glacial and interglacial periods. Then, the karst landforms in Nagura Bay would have been submerged for the final time during a period of postglacial sea level rise, with no subsequent rapid subsidence or uplift occurring in Nagura Bay since MIS-5e (Yamada et al., 2007).

5.4. Geomorphological features of submerged karst in Nagura Bay

Ishigaki Island can be considered a composite island based on the island type classification of the Carbonate Island Karst Model (Mylroie, 2013). For this island type, both carbonate and non-carbonate rocks are exposed at the surface and both allogenic and autogenic catchments are present. Allogenic streams have been shown to contribute to the enlargement of cave passages (Gunn, 2013). The present-day Nagura River flows through the non-carbonate rocks in its catchment (Fig. 1B). However, during the last glacial period, allogenic water may have entered the carbonate rocks in Nagura Bay and provided dissolutional potential for the formation of the transverse valleys of the fluviokarsts. Thus, the Nagura River may have been formed as a limestone gorge in the lower reaches of the river during the last glacial period.

Gunn (2004) suggested that fluviokarst can be considered as one end member in a continuous sequence of surface landform assemblages for carbonate rocks, where the other end member is polygonal karst, the entire surface of which is typically pitted by dolines with little or no trace of any previous valley form. These two end members seem to coexist in the submerged karst of Nagura Bay. Moreover, it is particularly remarkable that various landform assemblages spanning the sequence from dolines to polygonal karst and uvalas are present in Nagura Bay. The dolines in Nagura Bay exhibit either bowl-shaped forms or flat floors with vertical walls and have sizes that correspond to those of general karst dolines, which are typically tens to hundreds of meters in diameter and exhibit depths of a few meters to tens of meters (Williams, 2004). Their sizes are also similar to submerged dolines (observed by aerial photographs) in the Ogasawara Islands, southeastern Japan (Hori, 1996).

The cockpit landscape in Nagura Bay, which exhibits dominant depression/cone diameters of ~100–150 m, resembles the humid tropical type example of the “egg-box” morphology developed in polygonal karst at Cockpit Country in Jamaica (Day and Chenoweth, 2004), where the diameter of depressions and cones is approximately 200 m. In the Ryukyu Islands, a typical cockpit karst is developed in the Nakijin Limestone of the Triassic accretionary wedge of the Motobu Peninsula, Okinawa Island (Arakawa and Miura, 1990). The dominant diameters of cockpit depressions and conical hills are in the ranges 100–200 m and 50–100 m, respectively, in the Yamazato area (Fig. 8A, C). The porosity of the Nakijin Limestone is ~0%, whereas a porosity of 15.2–48.4% was observed for the Pleistocene limestone of the Ryukyu Group (Maekado, 1989). Matsukura et al. (2007) reported a corrosion rate of 205 mm ka^{-1} for a Pleistocene reef terrace. Because the porous limestone is more soluble, a slower corrosion rate is assumed for the Nakijin Limestone; this may have allowed long-term karstification to occur, thus developing the cockpit karst. Similarly, at Ishigaki Island, conical hills with horizontal scales of ~100–500 m (Fig. 8B, D) developed in the Eocene limestone (Miyara Formation) in the Hoshino area (Fig. 1B).

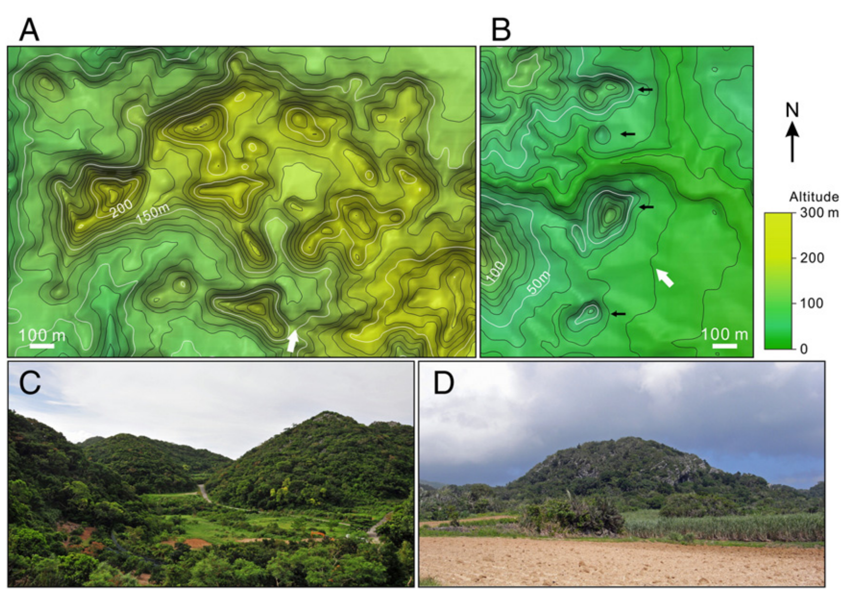

Fig. 8. Cone karsts in the Ryukyu Islands. (A, C) Yamazato area of the Motobu Peninsula, Okinawa Island. (B, D) The Hoshino area of Ishigaki Island. The maps were prepared using a 10 m mesh DEM published by the Geospatial Information Authority of Japan (http://www.gsi.go.jp) and visualized using IVS3D Fledermaus. Color scales show altitudes. Black arrows in (B) indicate limestone hills. Note that the entirety of (A) consists of limestone. White arrows in (A) and (B) indicate the direction of photography for (C) and (D), respectively. Photographs were taken by H. Kan.

The pentagonal polygonal karsts observed in Nagura Bay have many features in common with the polygonal karst in Papua New Guinea described by Williams (1971). In particular, all of the available space in these karst landscapes is occupied by depressions, rather like an egg box, and the topographic divides separating adjoining solution depressions exhibit polygonal patterns in plan view. Once a cellular polygonal karst has been established, its geometry typically undergoes only minor modification through time (Williams, 1972). In Nagura Bay, an uvala is located next to the dissected polygonal landform located in the B1 area (Fig. 3). These landforms may represent the corrosional sequence of polygonal karst. Meanwhile, the low-relief cockpit karsts found primarily in the most seaward part of Nagura Bay may indicate that the "egg-box" style of polygonal karst did not always develop to form pentagonal polygonal karst.

An aerial photograph (Fig. 9) illustrates that the submarine plateaus observed in our bathymetric result extend to the shallow coastal area of Nagura Bay, beyond the area covered by our bathymetric survey. Many closed depressions can also be seen in this photograph. For example, the shallow sea geomorphology of the river mouth is also formed by closed depressions. Thus, the entirety of Nagura Bay appears to exhibit characteristics consistent with those of submerged karst. Nagura Bay extends for 6 km and 5 km in the north–south and east–west directions, respectively. This is approximately the same size as Minami Daito Island in the northwestern Pacific and is larger than the limestone area of the Hiraodai Plateau, a typical karst area on Kyushu Island, Japan. Thus, Nagura Bay appears to be the largest submerged karst in Japan.

5.5. Perspectives on geological structure

Because the submerged karst in Nagura Bay was covered by reef structures, the host rock of the karst could not be identified during our SCUBA diving surveys. Thus, knowledge of this karstified rock remains lacking. The karst processes may affect not only limestone bedrock but also soluble evaporites. However, evaporites are not distributed in the Ryukyu Islands. Based on consideration of the geology of Ishigaki Island, the following strata are possible host rocks: (1) the Pleistocene limestone of the Ryukyu Group, (2) the Eocene limestone of the Miyara Formation, and (3) the limestone of the Permian Fusaki Formation.

The Pleistocene limestone of the Ryukyu Group (Ohama Formation) is distributed broadly on Ishigaki Island (Fig. 1B). It is a porous reef limestone composed of corals, foraminifers, and coralline algae, among other constituents. Cockpit karsts are typically developed in pure and hard carbonate strata without major impermeable layers (Zhu et al., 2013), and it is assumed that the landforms in Nagura Bay developed in solid limestone with low permeability, with dolines developed along joints. However, large karst features have not developed in the Pleistocene limestone areas of the Ryukyu Islands, where only collapsed dolines or dish-shaped shallow dolines have formed. Moreover, the cone karsts developed in areas consisting of the Pleistocene limestone of the Ryukyu Group typically appear as solitary cones (Hirose et al., 2013). We suggest that the porous Pleistocene limestone with high permeability would not have allowed the formation of the large karst features developed in Nagura Bay.

The limestone of the Permian Fusaki Formation is an accretionary wedge with a relatively limited surface distribution covering an area of ~0.05 km^2 (Fig. 1B). Thus, the submerged karst in Nagura Bay likely developed in the Eocene limestone of the Miyara Formation, which accumulated on the continental shelf and has not been deformed. This limestone is distributed widely throughout the terrestrial parts of Ishigaki Island: conical hills are developed in the Hoshino district on the eastern coast of the island, whereas karren are developed along the northwestern coast of Nagura Bay. Thus, we tentatively assume that the Miyara Formation limestone is the host rock of the submerged karst landscape in Nagura Bay.

Despite the presumed presence of a large limestone area underlying Nagura Bay, older (i.e., Tertiary or older) limestones are seldom found distributed on land near the bay (Fig. 1B). We interpret this as follows. In contrast to terrestrial areas, where karst corrosion has occurred

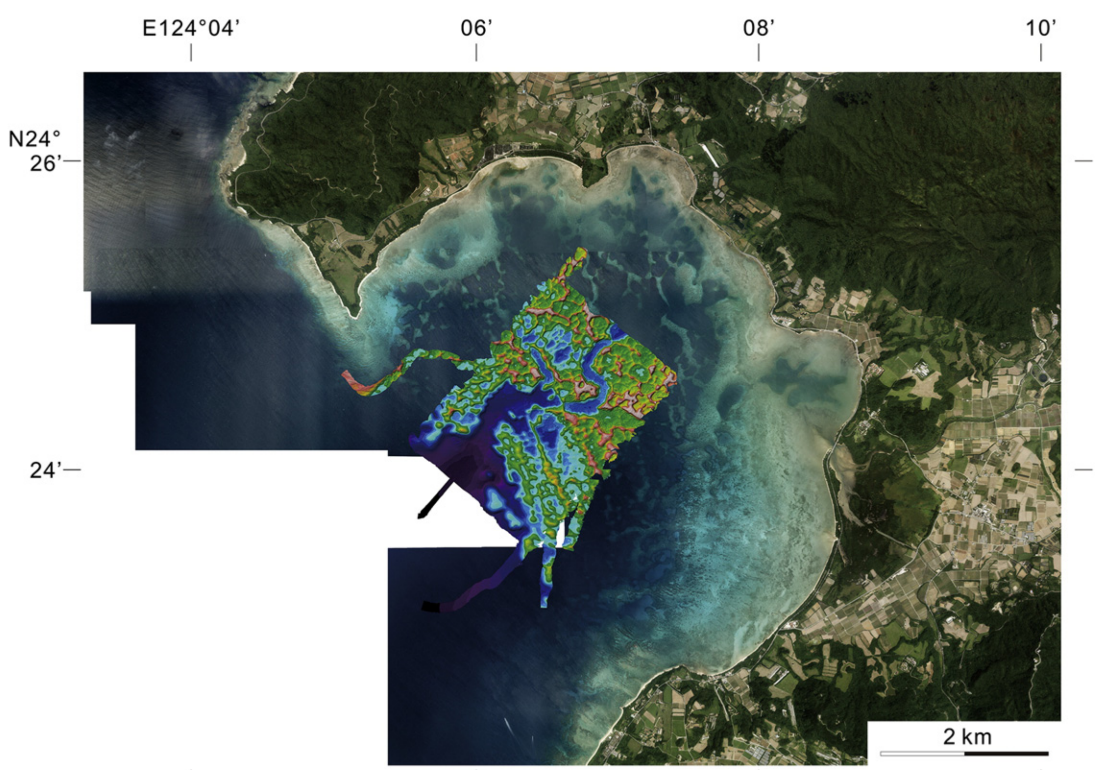

Fig. 9. Coastal geomorphology with reference to the bathymetric results showing submerged karst in Nagura Bay. The aerial photograph was provided by Pasco Co. Ltd.

continuously owing to subaerial exposure, karst in the tropical island shelf has experienced repeated accumulation of carbonate sediments due to submergence during interglacial periods. Corrosion that occurred during glacial periods presumably acted to remove the most recent deposits. However, the older limestones likely remained in the submerged karst on the island shelf and were less affected by corrosion.

The preliminary results of our latest ongoing drilling survey, which penetrated to 60 m drilling depth in the central submarine plateau between dolines d1 and d2 (Fig. 3), indicate that a considerable thickness (~34 m) of postglacial reef complex overlies the Pleistocene limestone. Although detailed analysis of this core has yet to be completed, these preliminary results show that this is the thickest record of postglacial reef obtained in the Ryukyu Islands to date.

Moreover, preliminary observations of Pleistocene stratigraphy in our drilling core indicate the presence of a layer of rigid in situ reef boundstone with a thickness of ~2 m, underlain by loose sediments consisting of Pleistocene limestone debris and soil down to a drilling depth of 60 m. We suspect that the Pleistocene limestone may be underlain by a dense rigid Tertiary limestone that constituted the original form of the submerged karst landforms. However, as we have not yet reached this older rigid limestone, our knowledge of the entire geological structure of the submerged karst in Nagura Bay remains incomplete.

In contrast to the relatively thin (~3 m) postglacial deposits covering submerged karst landforms reported in the Adriatic Sea (Taviani et al., 2012), the thick postglacial reef complex of Nagura Bay has accumulated on pre-existing landforms. These pre-existing prototypical landforms are assumed to be old and to lie at much deeper levels within the strata of the region. Subsequently, the undulations of landforms in this region may have been amplified by active reef growth, which typically occurs in convex topography during multiple interglacial periods, whereas the depressions have been buried by allochthonous reef sediments. Thus, the development of submerged karst landforms in tropical coral reef areas may be different in both style and history to those developed in temperate shelves.

6. Conclusions

We have discovered and visualized an extensive submerged karst landscape in Nagura Bay, Ishigaki Island, southwestern Japan, using multibeam bathymetric survey. Based on our bathymetric map with a grid size of 1 m, various types of humid tropical karst features coexist in the bay, including fluviokarst, doline karst, cockpit karst, polygonal karst, uvalas, and mega-dolines. The dominant spatial scale of the geomorphology observed in Nagura Bay is hundreds of meters, which is an order of magnitude larger than the present coral reef geomorphology at a similar depth.

The present marine conditions of Nagura Bay are characterized by low energy (calm sea) and low irradiance owing to the terrestrial influence. Such conditions have been emphasized by the presence of large undulating landforms, which cause decreases in wave intensity and irradiance with depth. These characteristics have acted to establish unique conditions compared to other coral reef areas in the Ryukyu Islands.

However, because the karst landforms are covered by a thick postglacial reef complex, the host rock remains unknown. We assume that Nagura Bay was a large karst basin in which older limestone remained submerged, thus preventing corrosion and the accumulation of reef sediments during periods of submersion, whereas the limestone outcropping on land was corroded during multiple interglacial and glacial periods. Based on our bathymetric result together with aerial photographs of the coastal area, we conclude that the submerged karst landscape has likely developed throughout the whole of Nagura Bay, covering an area of ~6×5 km. Accordingly, this area hosts the largest submerged karst in Japan.

Acknowledgment

This study was supported by the Japan Society for the Promotion of Science (JSPS) through a Grant-in-Aid for Scientific Research (A) (Nos. 22240084 and 25242026; chief investigator: H. Kan). The broadband multibeam echosounder (Sonic 2022) was introduced to HK's laboratory using the above-mentioned grant #22240084. We would also like to express our appreciation for Shin Takada and Kouichi Nakano of the Toyo Corporation for technical support with R2 Sonic 2022. Field surveys were supported by the following people: Tateru Yarabu and Minoru Uehara, who steered the research boat; Ken'ichi Togashi, who assisted with the SCUBA diving surveys; and Tsuguo Chimura of the Chuo Kaihatsu Co. Ltd., who assisted with the drilling survey. Akira Maekado kindly provided information regarding limestone corrosion in the Ryukyu Islands. The constructive comments of Davide Baioni and two anonymous reviewers and the editor Jo De Waele helped to improve this contribution.

References

Abby, E., Webster, J.M., Braga, J.C., Sugihara, K., Wallace, C., Iryu, Y., Potts, D., Done, T., Camoin, G., Seard, C., 2011. Variation in deglacial coralgal assemblages and their paleoenvironmental significance: IODP Expedition 310, "Tahiti Sea Level". Glob. Planet. Chang. 76, 1–15.

Arakawa, T., Miura, H., 1990. Karst landforms in Japan. In: Hori, N., Toguchi, K., Hasegawa, H., Nakai, T. (Eds.), Tropics in Japan: Natural History of Coral IslandsSeries of Coral Islands in Japan. 1. Kokon-shoin Ltd, Tokyo, pp. 215–229 (in Japanese).

Bak, R.P.M., Nieuwland, G., Meesters, E.H., 2005. Coral reef crisis in deep and shallow reefs: 30 years of constancy and change in reef of Curacao and Bonaire. Coral Reefs 24, 475–479.

Barnard, P.L., Erikson, L.H., Elias, E.P.L., Dartnell, P., 2013. Sediment transport patterns in the San Francisco Bay Coastal System from cross-validation of bedform asymmetry and modeled residual flux. Mar. Geol. 345, 72–95.

Barrie, J.V., Conway, K.W., Harris, P.T., 2013. The Queen Charlotte Fault, British Columbia: seafloor anatomy of a transform fault and its influence on sediment processes. Geo-Mar. Lett. 33, 311–318.

Beaman, R.J., Webster, J.D., Wust, R.A.J., 2008. New evidence for drowned shelf edge reefs in the Great Barrier Reef, Australia. Mar. Geol. 247, 17–34.

Bridge, T.C.L., Hughes, T.P., Guinotte, J.M., Bongaerts, P., 2013. Call to protect all coral reefs. Nat. Clim. Chang. 3, 528–530.

Burke, R.B., 1993. How have Holocene sea level rise and antecedent topography influenced Belize Barrier Reef development? Proc. Colloquium on Global Aspects of Coral Reefs. Univ. Miami, Miami, Florida, pp. 14–20.

Ćalić, J., 2011. Karstic uvala revisited: toward a redefinition of the term. Geomorphology 134, 32–42.

Camoin, G.F., Montaggioni, L.F., Braithwaite, C.J.R., 2004. Late glacial to post glacial sea levels in the Western Indian Ocean. Mar. Geol. 206, 119–146.

Collina-Girard, J., 1996. Préhistoire et karst littoral: la grotte Cosquer et les Calanques Marseillaises (Bouches-du-Rhône, France). Karstologia 27, 27–40 (re-published in English); Collina-Girard, J., 2004. Prehistory and coastal karst area: Cosquer Cave and the "Calamques" of Marseille. Speleogenesis and Evolution of Karst Aquifers. 2(2), pp. 1–13.

Daoxian, Y., 2013. Variation of karst geomorphology over geoclimatic gradients. In: Shroder, J.F., Frumkin, A. (Eds.), Treatise on Geomorphology 6. Academic Press, San Diego, CA, pp. 319–326.

Day, M., Chenoweth, S., 2004. Cockpit Country cone karst, Jamaica. In: Gunn, J. (Ed.), Encyclopedia of Caves and Karst Science. Fitzroy Dearborn, New York, pp. 233–235.

De Waele, J., Brook, G.A., Oertel, A., 2009. Monk seal (*Monachus monachus*) bones in Bel Torrente Cave (central-east Sardinia) and their paleogeographical significance. J. Cave Karst Stud. 71, 16–23.

Diekmann, B., Hofmann, J., Henrich, R., Fütterer, D.K., Röhl, U., Wei, K.-Y., 2008. Detrital sediment supply in the southern Okinawa Trough and its relation to sea-level and Kuroshio dynamics during the late Quaternary. Mar. Geol. 255, 83–95.

Dieter, K., 1991. Main trends of Palau Islands' coastal evolution, identified by air and ground truthing. GeoJournal 24, 77–85.

Ford, D., Williams, P., 2007. Karst Hydrogeology and Geomorphology. John Wiley & Sons Ltd., Chichester, (562p).

Foster, H.L., 1965. Geology of Ishigaki-shima Ryukyu-retto. U.S. Geological Survey, Professional Paper. 339A, pp. 1–119.

Fujimoto, K., Yamanouchi, H., Mezaki, S., Hasegawa, H., Maekado, A., 1995. Development of lowland and mangrove forest in Nagura River, Ishigaki Island. Proc. 47th General Meeting Association of Japanese Geographers, pp. 384–385 (in Japanese).

Fujita, K., Omori, A., Yokoyama, Y., Sakai, S., Iryu, Y., 2010. Sea-level rise during Termination II inferred from large benthic foraminifers: IODP Expedition 310, Tahiti Sea Level. Mar. Geol. 271, 149–155.

Goto, K., Miyagi, K., Kawamata, H., Imamura, F., 2010. Discrimination of boulders deposited by tsunamis and storm waves at Ishigaki Island, Japan. Mar. Geol. 269, 34–45.

Gunn, J., 2004. Fluviokarst. In: Gunn, J. (Ed.), Encyclopedia of Caves and Karst Science. Fitzroy Dearborn, New York, pp. 363–364.

Gunn, J., 2013. Denudation and erosion rates in karst. In: Shroder, J.F., Frumkin, A. (Eds.), Treatise on Geomorphology 6. Academic Press, San Diego, CA, pp. 72–81.

Harris, M.S., Sautter, L.R., Johnson, K.L., Luciano, K.E., Sedberry, G.R., Wright, E.E., Siuda, A.N.S., 2013a. Continental shelf landscapes of the southern United States since the last interglacial. Geomorphology 203, 6–24.

Harris, P.T., Bridge, T.C.L., Beaman, R.J., Webster, J.M., Nichol, S.L., Brooke, B.P., 2013b. Submerged banks in the Great Barrier Reef, Australia, greatly increase available coral reef habitat. ICES J. Mar. Sci. 70, 284–293.

Hirose, T., Sangawa, T., Aoki, H., Matsukura, Y., Maekado, A., 2013. A study of cone karsts developed on Quaternary Ryukyu Limestone in Okinawa. Okinawa J. Geogr. Stud. 12, 25–32 (in Japanese).

Hongo, C., Kayanne, H., 2009. Holocene coral reef development under windward and leeward locations at Ishigaki Island, Ryukyu Islands, Japan. Sediment. Geol. 214, 62–73.

Hori, N., 1996. Submerged karst topography around Minami-Shima and Minami-Saki Chichijima, Ogasawara Islands. In: Nakamura, K., Ujiié, H., Ikehara, S., Tagawa, H., Hori, N. (Eds.), Nature in Japan. 8. Iwanami Shoten, Tokyo, pp. 86–87 (in Japanese).

Howe, J.A., Dove, D., Bradwell, T., Gafeira, J., 2012. Submarine geomorphology and glacial history of the Sea of the Hebrides, UK. Mar. Geol. 315–318, 61–76.

Ikeda, S., Osawa, K., Akamatsu, Y., 2009. Sediment and nutrients transport in watershed and their impact on coastal environment. Proc. Jpn. Acad. Ser. B 85, 374–390.

Iryu, Y., Matsuda, H., 2010. Neogene and Quaternary, Ryukyu Islands. In: Geological Society of Japan (Ed.), Regional geology of Japan. 8. Asakura Shoten, Tokyo, pp. 149–154 (in Japanese).

Iryu, Y., Nakamori, T., Yamada, T., 1998. Pleistocene reef complex deposits in the Central Ryukyus, south-western Japan. In: Camoin, G.F., Davies, P.J. (Eds.), Reefs and Carbonate Platforms in the Pacific and Indian Oceans. Special Publication of the International Association of Sedimentologists. 25, pp. 197–213.

Ishigakijima Local Meteorological Observatory, 2013. http://www.jma-net.go.jp/ishigaki/index.html (accessed on November 2013).

Isozaki, Y., Nishimura, Y., 1989. Fusaki Formation, Jurassic subduction–accretion complex on Ishigaki Island, southern Ryukyus and its geologic implication to Late Mesozoic convergent margin of East Asia. Mem. Geol. Soc. Jpn. 33, 259–275 (in Japanese with English abstract).

Japan Meteorological Agency, 2013. http://www.jma.go.jp (accessed on November 2013).

Jennings, J.N., 1985. Karst Geomorphology. Basil Blackwell, Oxford, UK, (293 pp).

Kan, H., 2011. Ryukyu Islands. In: Hopley, D. (Ed.), Encyclopedia of Modern Coral Reefs: Structure, Form and Process, Encyclopedia of Earth Science Series. Springer, Dordrecht, pp. 940–945.

Kan, H., Kawana, T., 2006. 'Catch-up' of a high-latitude barrier reef by back-reef growth during post-glacial sea-level rise, Southern Ryukyus, Japan. Proc. 10th International Coral Reef Symposium, Okinawa, Japan, pp. 494–503.

Kan, H., Hori, N., Ichikawa, K., 1997. Formation of a coral reef-front spur. Coral Reefs 16, 3–4.

Kiernan, K., 1994. The coastal tower karst of Phang Nga Bay. International Symposium on the Exploitation and Protection of Karst and Cave Scenic Tourist Resources: Study of Karst and Cave Scenic Tourist Resources. University of Tasmania ePrints, pp. 9–21.

Kitamura, A., Yamamoto, N., Kase, T., Ohashi, S., Hiramoto, M., Fukusawa, H., Watanabe, T., Irino, T., Kojitani, H., Shimamura, M., Kawakami, I., 2007. Potential of submarine-cave sediments and oxygen isotope composition of cavernicolous micro-bivalve as a late Holocene paleoenvironmental record. Glob. Planet. Chang. 55, 301–316.

Lehmann, H., 1936. Morphologische studies auf Java. Series 3, No. 9, GeographischeAbhandlungen, Stuttgart, Germany, (114 pp).

Lesser, M.P., Slattery, M., Leichter, J.J., 2009. Ecology of mesophotic coral reefs. J. Exp. Mar. Biol. Ecol. 375, 1–8.

Li, M.Z., Shaw, J., Todd, B.J., Kostylev, V.E., Wu, Y., 2014. Sediment transport and development of banner banks and sandwaves in an extreme tidal system: Upper Bay of Fundy, Canada. Cont. Shelf Res. 83, 86–107.

Macintyre, I.G., Precht, W.F., Aronson, R.B., 2000. Origin of the Pelican Cay Ponds, Belize. Atoll Res. Bull. 466, 1–11.

Maekado, A., 2000. Some physical and mechanical properties of the limestones in Okinawa Island. Bulletin of the Okinawa Geographical Society 2, 29–33.

Matsukura, Y., Maekado, A., Aoki, H., Kogure, T., Kitano, Y., 2007. Surface lowering rates of uplifted limestone terraces estimated from the height of pedestals on a subtropical island of Japan. Earth Surf. Process. Landf. 32, 1110–1115.

Micallef, A., Foglini, F., Le Bas, T., Angeletti, L., Maselli, V., Pasuto, A., Taviani, M., 2013. The submerged paleolandscape of the Maltese Islands: morphology, evolution and relation to Quaternary environmental change. Mar. Geol. 335, 129–147.

Mishima, M., Kawahata, H., Suzuki, A., Inoue, M., Okai, T., Omura, A., 2009. Reconstruction of the East China Sea palaeoenvironment at 16 ka by comparison of fossil and modern Faviidae corals from the Ryukyus, southwestern Japan. J. Quat. Sci. 24, 928–936.

Miyagi, T., Ajiki, K., Fujimoto, K., 2003. Mangrove Habitat Dynamics and Human Relation. Kokon-Shoin Ltd., Tokyo, (193 pp) (in Japanese).

Mylroie, J.E., 2013. Coastal karst development in carbonate rocks. In: Lace, M.J., Mylroie, J.E. (Eds.), Coastal Karst Landforms, Coastal Research Library. 5. Springer, Dordrecht, pp. 77–109.

Mylroie, J.E., Mylroie, J.R., 2013. Flank margin caves in carbonate islands and the effects of sea level. In: Shroder, J.F., Frumkin, A. (Eds.), Treatise on Geomorphology 6. Academic Press, San Diego, CA, pp. 351–362.

Nagao, M., Kan, H., Nakano, K., Takada, S., Ogasawara, H., Nakamura, T., Ohashi, T., Suzuki, A., 2011. An attempt to find small artificial objects in the shallow sea bottom using a broadband multibeam echosounder. Proceedings of International Sessions in Conference on Coastal Engineering JSCE. 2, pp. 51–55.

Nakae, S., Nagamori, H., Miyazaki, K., Komazawa, M., 2009. Geological Map of Japan 1: 200,000, Ishigaki Jima. Geological Survey of Japan, AIST, Tsukuba (in Japanese with English abstract).

Nakamori, T., 1986. Community structures of Recent and Pleistocene hermatypic corals in the Ryukyu Islands, Japan. The Science Reports of the Tohoku University, 2nd Series (Geology) 56, 71–133.

Nakamori, T., Iryu, Y., Yamada, T., 1995. Development of coral reefs of the Ryukyu Islands (southwest Japan, East China Sea) during Pleistocene sea-level change. Sediment. Geol. 99, 215–231.

Nature Conservation Bureau, Ministry of the Environment, 2002. Annual report of coral reef monitoring around Ishigaki Island 2002 Japan (in Japanese).

Paskoff, R.P., 2005. Karst coasts. In: Schwartz, M.L. (Ed.), Encyclopedia of Coastal Science. Springer, Dordrecht, pp. 581–586.

Purdy, E.G., 1974. Karst-determined facies patterns in British Honduras: Holocene carbonate sedimentation model. AAPG Bull. 58, 825–855.

Purdy, E.G., 1998. Structural termination of the southern end of the Belize Barrier Reef. Coral Reefs 17, 231–234.

Purkis, S.J., Rowlands, G.P., Riegl, B.M., Renaud, P.G., 2010. The paradox of tropical karst morphology in the coral reefs of the arid Middle East. Geology 38, 227–230.

Rasmussen, K.A., Neumann, A.C., 1988. Holocene overprints of Pleistocene paleokarst: bight of Abaco, Bahamas. In: James, N.P., Choquette, P.W. (Eds.), Paleokarst. Springer-Verlag, New York, pp. 132–148.

Sasaki, K., Omura, A., Miwa, T., Tsuji, Y., Matsuda, H., Nakamori, T., Iryu, Y., Yamada, T., Sato, Y., Nakagawa, H., 2006. ^{230}Th/^{234}U and ^{14}C dating of a lowstand coral reef beneath the insular shelf off Irabu Island, Ryukyus, southwestern Japan. Island Arc 15, 455–467.

Scheffers, A.M., Scheffers, S.R., Kelletat, D.H., 2012. The Coastlines of the World With Google Earth. Springer, Dordrecht, (293p).

Sibuet, J.-C., Letouzey, J., Barbier, F., Charvet, J., Foucher, J.-P., Hilde, T.W.C., Kimura, M., Ling-Yun, C., Marsset, B., Muller, C., Stéphan, J.-F., 1987. Back arc extension in the Okinawa Trough. J. Geophys. Res. 92, 14041–14063.

Slattery, M., Lesser, M.P., Brazeau, D., Stokes, M.D., Leichter, J.J., 2011. Connectivity and stability of mesophotic coral reefs. J. Exp. Mar. Biol. Ecol. 408, 32–41.

Surić, M., 2002. Submarine karst of Croatia — evidence of former lower sea levels. Acta Carsologica 31 (3), 89–98.

Surić, M., Lončarić, R., Lončar, N., 2010. Submerged caves of Croatia: distribution, classification and origin. Environ. Earth Sci. 61, 1473–1480.

Taviani, M., 1984. Submarine 'sinkholes': a review. Proc. First Multidiciplinary Conference on Sinkholes, Orlando, Florida, USA, pp. 117–121.

Taviani, M., Angeletti, L., Campiani, E., Ceregato, A., Foglini, F., Maselli, V., Morsilli, M., Parise, M., Trincardi, F., 2012. Drowned karst landscape offshore the Apulian margin (Southern Adriatic Sea, Italy). J. Cave Karst Stud. 74, 197–212.

Tibor, G., Niemi, T.M., Ben-Avraham, Z., Al-Zoubi, A., Sade, R.A., Hall, J.K., Hartman, G., Akawi, E., Abueladas, A., Al-Ruzouq, R., 2010. Active tectonic morphology and submarine deformation of the northern Gulf of Eliat/Aqaba from analyses of multibeam data. Geo-Mar. Lett. 30, 561–573.

Tsuburaya, H., Sato, T., 1985. Borehole of MITI Miyakojima-Oki. J. Jpn. Assoc. Pet. Technol. 50, 25–33 (in Japanese).

Ujiié, H., 1996. Formation of the foundation of Ryukyu Island Arc. In: Nakamura, K., Ujiié, H., Ikehara, S., Tagawa, H., Hori, N. (Eds.), Nature in Japan. 8. Iwanami Shoten, Tokyo, pp. 93–111 (in Japanese).

Ujiié, Y., Ujiié, H., 2006. Dynamic changes of the surface and intermediate waters in the Ryukyu Arc region during the past ~250,000 years: based on planktonic and benthic foraminiferal analyses of two IMAGES cores. Fossils 79, 43–59.

Waltham, T., Hamilton-Smith, E., 2004. Ha Long Bay, Vietnam. In: Gunn, J. (Ed.), Encyclopedia of Caves and Karst Science. Fitzroy Dearborn, New York, pp. 413–414.

Webster, J.M., Clague, D.A., Braga, J.C., Spalding, H., Renema, W., Kelley, C., Applegate, B., Smith, J.R., Paull, C.K., Moore, J.G., Potts, D., 2006. Drowned coralline algal dominated deposits off Lanai, Hawaii; carbonate accretion and vertical tectonics over the last 30 ka. Mar. Geol. 225, 223–246.

Williams, P.W., 1971. Illustrating morphometric analysis of karst with examples from New Guinea. Z. Geomorphol. 15, 40–61.

Williams, P.W., 1972. Morphometric analysis of polygonal karst in New Guinea. Geol. Soc. Am. Bull. 83, 761–796.

Williams, P., 2004. Dolines. In: Gunn, J. (Ed.), Encyclopedia of Caves and Karst Science. Fitzroy Dearborn, New York, pp. 304–310.

Yamada, S., Matsuda, H., Omura, A., 2007. Uranium-series dates of fossil hermatypic corals in Ishigaki-jima Island, Okinawa Prefecture, and their significance. J. Geol. Soc. Jpn. 113, 19–22 (in Japanese with English abstract).

Yamano, H., Kayanne, H., Yonekura, N., 2001. Anatomy of a modern coral reef flat: a recorder of storms and uplift in the late Holocene. J. Sediment. Res. 71, 295–304.

Yamano, H., Sugihara, K., Watanabe, T., Shimamura, M., Hyeong, K., 2012. Coral reefs at 34°N, Japan: exploring the end of environmental gradients. Geology 40, 835–838.

Yokoyama, Y., Lambeck, K. De, Deckker, P., Johnstone, P., Fifield, I.K., 2000. Timing of the Last Glacial Maximum from observed sea-level minima. Nature 406, 713–716.

Zhu, X., Zhu, D., Zhang, Y., Lynch, E.M., 2013. Tower karst and cone karst. In: Shroder, J.F., Frumkin, A. (Eds.), Treatise on Geomorphology 6. Academic Press, San Diego, CA, pp. 327–340.